Greece is past its COVID-19 epidemic peak, now entering asymptotic decay and ending its 42-day country-wide lockdown

Harris V. Georgiou (MSc,PhD)[a]

[a]Data Science Lab[1], University of Piraeus[2], Greece

Version: 1.0.00 – Last update: May 10, 2020

This work is a status update over a previous report (1) published in mid-April, regarding the COVID-19 epidemic at the national level for Greece, including SEIQRDP model identification and other data analytics, using the open-source datasets that were available at the time. In this report, these models are revisited and their validity is confirmed, based on the more recent up-to-date datasets from the two weeks that followed. Additionally, some problems are identified and addressed regarding the under-reporting of infections and delayed reporting of recovered cases. All models indicate that the national outbreak in Greece is now in recession, with a fade-out period of about 2-3 months, i.e., well within the summer, assuming no second-wave outbreak in the meantime. Provided the gradual deactivation of strong mitigation measures, the re-opening of international travelling and the summer holidays period, very intense and accurate tracking of the infections is required in Greece and every other country.

COVID-19 | SARS-CoV-2 | data analytics | SEIR | Greece

Recent experience from the evolution of the COVID-19 pandemic throughout the world has pushed the international interest of research teams from various fields and disciplines into rapid action, including Data Analytics for Epidemics.The main goal for such works is three-fold: (a) assemble, organize and present proper datasets, (b) formulate the dynamics of the outbreak by model identification, (c) validate the results and make sure we are better prepared for the next time. It is remarkable how much R&D work was accomplished in so little time - thousands of research papers and technical reports, most of them made available immediately to the entire world via open-access, in order for others to build upon them as quickly as possible. This is probably the first time the humanity was able to track a pandemic in almost real time, with huge amounts of information and data visualizations, available to everyone.

This work is a status update over a previous report (1) published on April 15th, regarding the evolution of the COVID-19 outbreak in Greece as the national epidemic had just passed its rising inflection point (change of curvature, i.e., 'slowing down') and stepping towards its peak. Now, about three weeks later, the epidemic models and data analytics presented there are revisited, re-evaluated and assessed regarding their accuracy and effectiveness in capturing the dynamics of the outbreak. It is extremely important to do so at this point, since Greece now seems to be entering the long period of asymptotic decay or 'fading-out' of the outbreak at the national level and just starting to gradually deactivating the mitigation measures of a country-wide lockdown that lasted 42 days.

1. New information about the virus

The latest results from clinical studies, monitoring of confirmed COVID-19 cases throughout the world, as well as model re-estimations with updated models during the past 2-3 weeks have revealed several new aspects of the SARS-CoV-2 virus, its pathology, how it attacks human cells and how it evolves into a potentially lethal disease, not only related to the lungs, but in relation to other organs too. New evidence (2) suggests that the virus may have already appeared in France as early as December 2019, i.e., a month before the country's first confirmed case was reported and only few weeks after 'patient zero' was admitted to a hospital in Wuhan, China. Additionally, there is evidence of a new strain of the virus*, still unconfirmed and non-verified†, which seems to have become dominant world-wide after February and seems to be more contagious than the versions that spread in the early days of the COVID-19 pandemic (3).

Figure 1 illustrates a general overview of the attack process of the virus, according to the latest information (4). The virus

*'Scientists say a now-dominant strain of the coronavirus could be more contagious than original' – L.A. Times (5-May-2020)

†'The Problem With Stories About Dangerous Coronavirus Mutations' – The Atlantic (6-May-2020)

Significance Statement

The overall short-term outlook for Greece continues to be towards positive. Peak active infections was realized on April 20-21st (1,856-1,860). There is a very strong delay in reporting recoveries, thus producing very large periods of missing data. Regardless, numbers for deaths and ICU used show ratios well within the world-wide estimations. The number of deaths related to COVID-19 is expected to be limited to 170 by the end of July. The basic reproduction number is confirmed to be $R_0 < 0.45$ and decreasing. If no second-wave outbreak is realized, the national outbreak is expected to fade out within August. Under-reporting of infections in Greece is revisited, with models showing that the effective factor seems to be no more than 1:3, at least for the clinically important cases of COVID-19; this may be up to 1:10 if patients with mild or no symptoms are included. Simulations show that a second-wave outbreak in Greece beginning right after the gradual deactivation of strong mitigation measures can still produce a five-fold epidemic intensity by mid-summer.

[1]Data Science Lab – http://datastories.org

[2]University of Piraeus, Greece – http://www.unipi.gr

[3]Corresponding author E-mail: hgeorgiou@unipi.gr

seems to exploit ACE2 receptors to attach onto and then break its 'spike' proteins, thus making it easier for its membrane to 'fuse' onto the host cell's membrane. Then, the virus injects its RNA into the host cell, exploiting the normal replication mechanism for its own replication, producing several more copies of the virus.

Regarding the pathology, there are several COVID-19 cases of young children and infants in France with multi-organ inflammations of unknown mechanism in relation to the virus and with symptoms similar to the Kawasaki disease[‡]. At least two such cases have been reported in Greece too[§]. Additionally, the actual probability of transmission of the virus outdoors and in spaces with effective open-air ventilation seems to be extremely low in practice[¶]. Recent evidence (5) shows that recovered patients probably gain antibodies to SARS-CoV-2, but the effective period is still unconfirmed. Research efforts are intensified more and more towards producing rapid testing methods, reliable and efficient treatments for patients, as well as a much-anticipated artificial immunization process via a safe vaccine (6, 7).

2. Timeline update for Greece

Since March 23rd, Greece was in strict lockdown in almost every aspect of everyday activities, from drastic reduction of international flights in and out of the country to very strict constraints on people's movements and gatherings. After a few days of uncertainty, mostly due to the incubation period of the virus in asymptotic carriers (8, 9), the lockdown seems to have played a major role in severely slowing down the spread of the virus in the general population.

Since mid-April when the previous report (1) was published, the most notable event is probably the emergence of one high-intensity infection cell in a private clinic in Athens. Starting from April 24th, 37 confirmed infections and three deaths related to COVID-19 were identified within almost a single day, due to lack of prompt testing and proper protective measures. The clinic was in central Athens and could become an infection super-spreader hub, if it remained undetected for another 2-3 days. Fortunately, the clinic and all patients and personnel were isolated, the facilities were sterilized and its functionality (hemodialysis centre) remained under very close monitoring in the following days.

According to the officials, the single most important mitigation measure for slowing down the outbreak, especially during the rapid rising of infections towards the peak, was explicit social distancing. Although exact estimations are still difficult to verify at this point for Greece (more data will become available later on), this effect seems to be supported by the experience from other countries (10), as Figure 2 illustrates for the UK. Publicly available data at the national level are not of sufficient quality at this point to verify all the daily estimations, the scientific committee in Greece has officially stated that the *basic reproduction number* R_0 has decreased steadily since the onset of the country-wide lockdown, from $R_0 \approx 4$ on March 13th to somewhere between $0.40 < R_0 < 0.45$ on April 30th. During the daily briefing on May 4th, the committee stated that 'R_0 is now far below 0.5, with probability 98.5%'[‖].

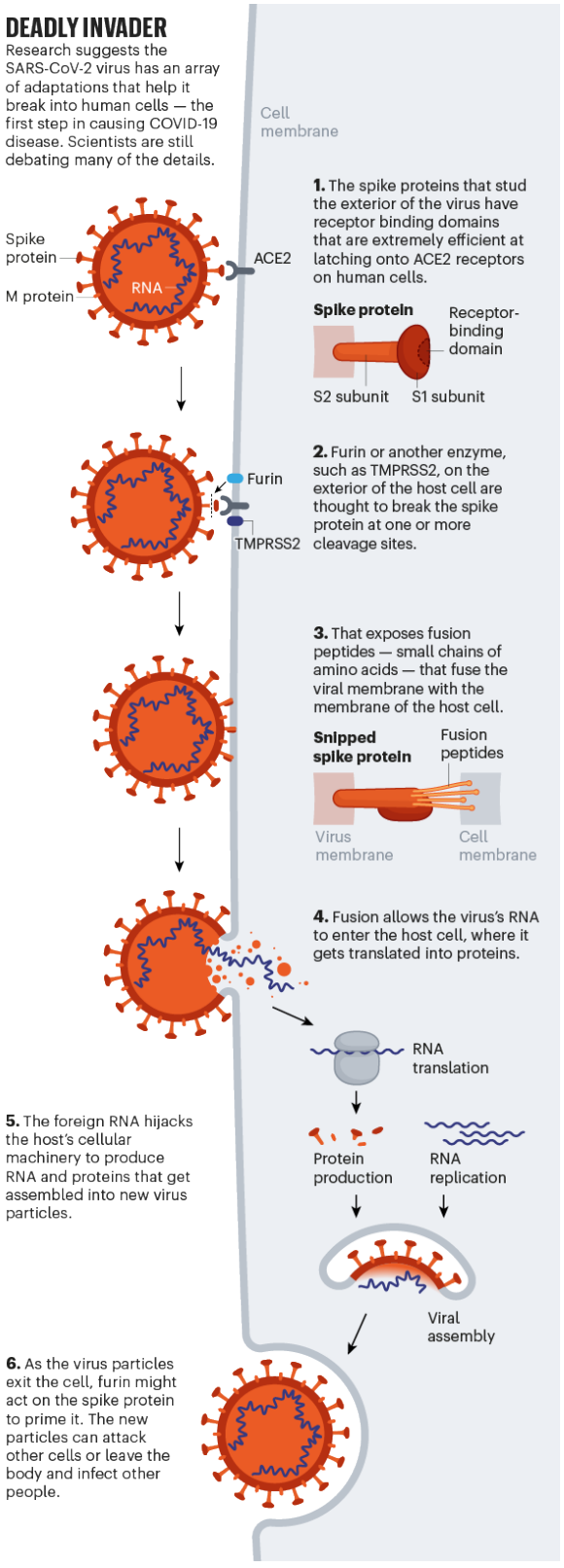

Fig. 1. General overview of the attack process of the SARS-CoV-2 virus (4).

[‡] 'Kawasaki disease' – Mayo Clinic (7-May-2020).
[§] 'Two children with Kawasaki symptoms in Greek hospitals' (in Greek) (7-May-2020).
[¶] 'Risk of transmitting COVID-19 outdoors is 'negligible' says health officer' (30-Apr-2020).
[‖] https://youtu.be/fzZEcWPsDGw?t=2301

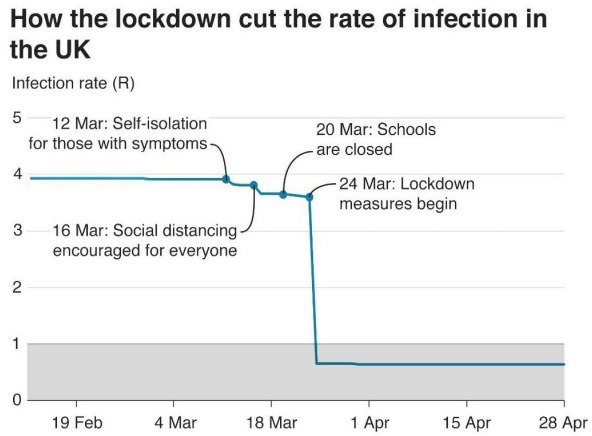

Fig. 2. Effects of explicit social distancing (lockdown) to the basic reproduction number R_0 in the UK (Source: Imperial College / Credits: BBC).

Fig. 3. COVID-19 heatmap of confirmed cases of infections in Greece on May 2nd, 2020 (Source: WHO).

Following a highest-value in active infections at around April 20th as expected and a gradual diffusion in the days that followed, it was decided that the outbreak had actually moved beyond its peak and into the beginning of the resolution phase. Hence, the scientific advisory committee and the Civil Protection agreed that gradual deactivation of the country-wide lockdown can be planned and implemented, starting from May 4th.

Figure 3 presents the heat map of confirmed cases of infections in Greece on May 2nd. Compared to the corresponding heat map from March 15th (1), there are only very few regions of higher-than-average infections rate, with the outbreak now diffused throughout the entire country.

3. Outbreak status in Greece

In order to analyze the progress of the outbreak in Greece, a detailed dataset of daily reports must be used. More specifically, the base dataset used in this study is the one provided

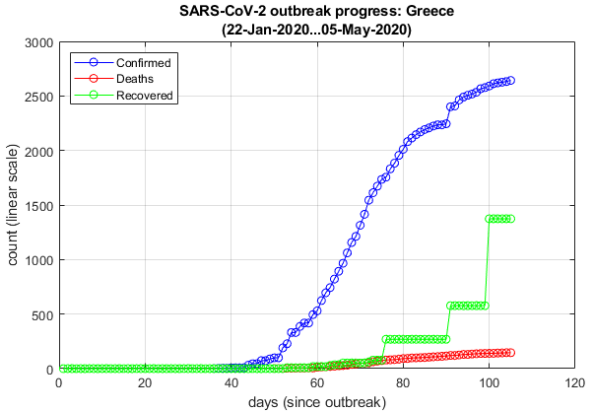

Fig. 4. Greece: Infected $I(t)$, Deaths $D(t)$ and Recovered $R(t)$, in linear scale.

for open-access** and updated on a daily basis by John Hopkins CSSE (11), which is the most popular and reliable source at the moment. It includes confirmed cases of Infected $I(t)$, Deaths $D(t)$ and Recovered $R(t)$, registered per-country and in some cases per-province/region/state, collected by the official sources from WHO, CDC (US), European CDC, state authorities in each country, as well as other open-access sources. Another source with regional data and access via API (12) was explored in this report, recently introduced and maintained by a volunteer team†† that is already collaborating with a number of research groups in Greece.

The basic curves for Greece from the beginning of the national epidemic are presented in Figures 4 and 5, in linear and logarithmic scale, respectively. From the basic curves, especially the $I(t)$, it is clear that the progress of the outbreak in Greece is exponential, as expected, but with a relatively slow rate. In the first two weeks there are several step-wise 'pauses' and 'bursts', as it is usually observed in the early stages of a fast-growing epidemic. This is due to the fact that the set sizes are still relatively small and statistics still unstable, as well as the lack of strict mitigation measures that are usually activated with some delay. Figure 6 presents a smoothed version of the I(t) series up to May 2nd, with indications of daily increases.

Two critical 'necks' before large increases in new infections seem to be around day 43 and day 51 since the start of the time series, i.e., March 4th and March 12th, respectively. These dates coincide with two important events in the Greek timeline: (a) the 1st confirmed case in the group of tourists who returned from Israel & Egypt and (b) 10 new confirmed cases of unknown origin and the 1st virus-associated death. For (a) it was understood that this group of tourists were asymptomatic for a few days and, thus, have been spreading the virus in the general population in the meantime, as the data proved subsequently. For (b) it was clear that the new confirmed cases of unknown origin, i.e., unrelated to both the group of tourists from Israel & Egypt as well as the other group that returned from northern Italy a few days earlier, were to increase rapidly, as was indeed the case. This is particularly important, because at this point it is understood that the virus has escaped the strict and detailed backtracing of infections and their close encounters, in order to impose targeted isolations. Thus,

** https://github.com/CSSEGISandData/COVID-19
†† COVID-19 Response Greece – https://www.covid19response.gr/

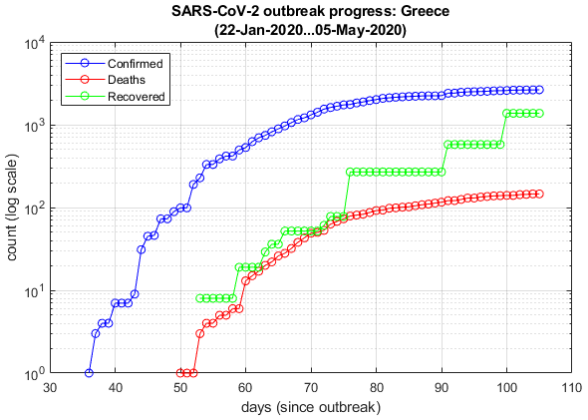

Fig. 5. Greece: Infected $I(t)$, Deaths $D(t)$ and Recovered $R(t)$, in logarithmic scale.

the operational plan should change to wide-range mitigation measures, as quickly as possible. Fortunately, this is what happened in the following days and, given that the outbreak continued to spread at a fast rate, Greece went into a nation-wide lockdown 11 days later. Another large 'step' in daily increase (+156) of confirmed cases is now evident on April 21st, which may be partially attributed to the detection of a the high-intensity infection cell in a private clinic in Athens three days later, as described previously in section 2.

A. Comparison to other countries. Taking into account the progress of the pandemic world-wide since early January 2020, the curves in Figures 4 and 5 reveal that Greece had a slow start. However, it is not sufficient to simply align the offset of each country's specific event to the others', e.g., the first reported death or the 100th confirmed case of COVID-19. The entire curve has to be compared and 'aligned' to others for a more realistic match. For this reason, Dynamic Time Warping (DTW) (13, 14) with Euclidean distance (see section 4.D for more details) was used for comparing Greece's infections $I(t)$ curve to countries in the general region of Europe and central/eastern Mediterranean Sea, especially those in direct 'contact' with Greece via international flights.

As described in the previous report (1), the DTW matching provides two important parameters for further study: (a) a more realistic estimate of the time offset for temporal alignment and (b) a DTW-based Euclidean distance that can be used as a similarity measure. Figure 7 illustrates the updated relative temporal difference (offset) of Greece-versus-others regarding the confirmed cases of infections $I(t)$. From this new DTW analysis it is evident that Greece is now fully 'synchronized' with the progress of the epidemic in the general region and its neighbours, now with a positive +0.51 days reference offset instead of -1.47 days previously reported for April 14th, and still closely 'aligned' temporally with North Macedonia and Estonia.

4. Data-driven analytics

Using the daily time series for confirmed cases of Infected $I(t)$, Deaths $D(t)$ and Recovered $R(t)$ in Greece, as well as data for ICU[‡‡] admissions, appropriate approximations can be developed in order to estimate important parameters of the outbreak in Greece.

[‡‡] ICU: Intensive Care Unit, typically a hospital bed with full quarantine and O2/ventilator capacity.

Table 1. LSE-optimal function parameters in Eq.1 for Greece. Upper half refers to data up to April 14th, lower half refers to data up to May 3rd.

Parameter	optim.value	conf.interval
a	8.097	(7.974, 8.221)
b	8.722	(8.420, 9.024)
c	0.064	(0.060, 0.068)
a	7.986	(7.941, 8.030)
b	8.787	(8.517, 9.058)
c	0.068	(0.065, 0.070)

Note: b and c are used with a negative sign in Eq.1. All confidence intervals are calculated for $p = 0.95$. Goodness-of-fit: R^2=0.992, RMSE=0.017

A. Infections. Using the $I(t)$ data series the following exponential formulation can be designed according to Eq.1 (1):

$$I(t) \approx e^{a-be^{-ct}} \quad [1]$$

where a, b, c are the function parameters. Their best-fit optimal values in the least-squares (LSE) sense (15) and the 95% confidence intervals for Greece are presented in Table 1. The first set of parameters (upper half) refers to the best-fit values with data up to April 14th (1), while the second set (lower half) refers to the updated best-fit values including all data up to May 3rd. It is clear that the updated model is almost identical to the previous one.

It should be noted that, although the plot in Figure 6 seems purely logistic-like ('sigmoid') (16) $y = L/(1+e^{-k(x-x_0)})$, Figures 4 and 5 reveal that at the start of the outbreak there may be a sharp exponential increase after a near-linear progression period, i.e., at the beginning of high-rate virus spreading in the general population and before the lockdown measures are activated. Therefore, although $I(t)$ here is the cumulative number as with $D(t)$ and $R(t)$ in similar well-fitted approximations, the logistic-like assumption for $I(t)$ is valid for its middle (inflection) and rightmost (saturation) sections, but may not be well-fitted for its leftmost (high-rate rising) section. This observation may provide better estimations on the saturation value of $I(t)$, which for $t \to \infty$ and $\alpha \approx 8$ gives $\lim_{t\to\infty} I(t) = e^{\alpha} \leq 3,000$ cases; still, a more reliable number for the saturation value is the one provided by SEIQRDP projections, as described later on in section 6.

B. Recovered, Deaths. One thing that is clearly evident from the publicly available epidemic data for Greece, especially for the period after mid-April, is the severe delay in reporting the recovered $R(t)$ daily values. From Figures 4 and 5 this can be easily observed for $R(t)$ (green), where there are multiple periods of no change at all, most notably two no-reporting periods of 15 days between 6-20 April (269) and 9 days subsequently between 21-29 April (577), as well as in the subsequent weeks. This constitutes a major issue in terms of data quality and, in turn, create significant difficulties in producing accurate and well-fitted epidemic models. Although this is a common observation in large-scale epidemics especially during in the period close to the peak of infections, it is not yet clear why

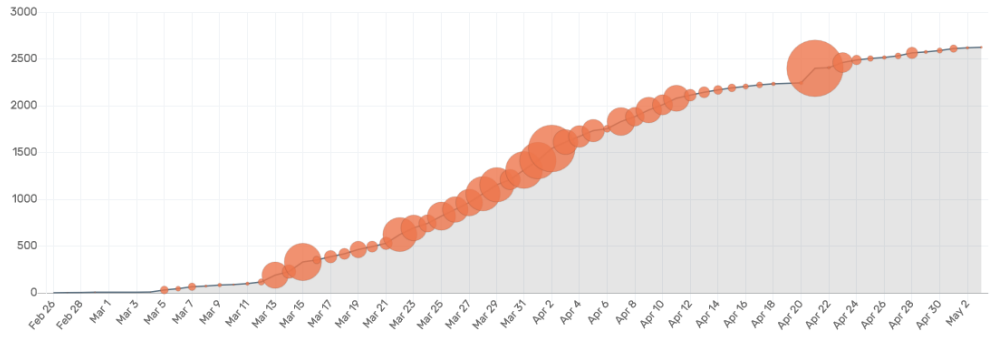

Fig. 6. Greece: Infected $I(t)$ sum (curve) and magnitude of daily increases (circles), update: May 2nd (Source: WHO, NPHO-Greece).

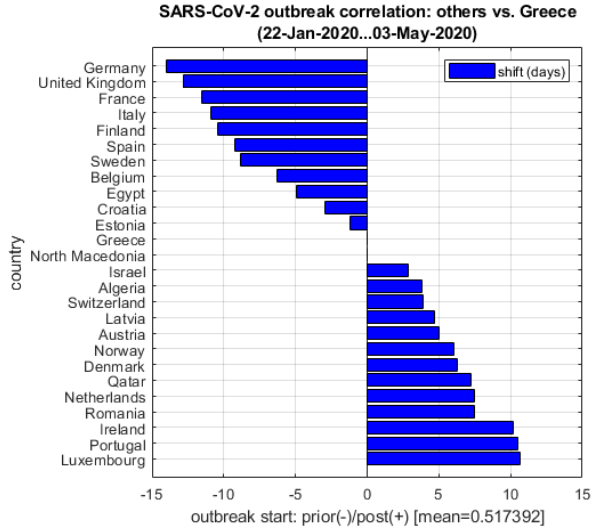

Fig. 7. DTW-based temporal offsets of Greece-versus-others regarding the confirmed infections $I(t)$.

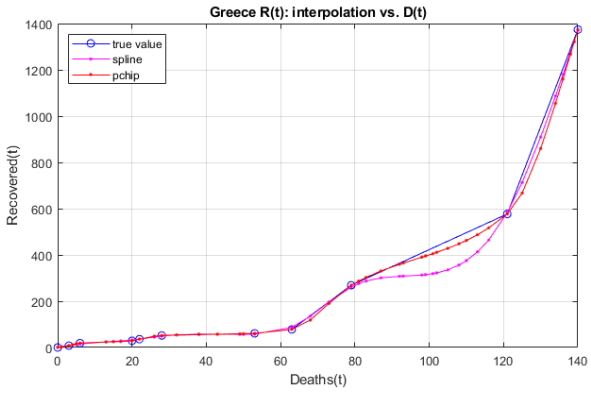

Fig. 8. Interpolation $\hat{R}(t)$ of Recovered $R(t)$ against Deaths $D(t)$.

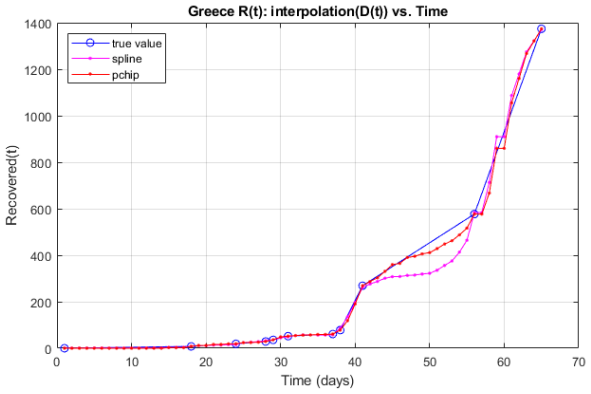

Fig. 9. Interpolation $\hat{R}(t)$ of Recovered $R(t)$ against time (t).

this effect was so severe in Greece with a relatively low number of active infections at the peak.

In order to cope with such quality degradation of the epidemic data, an additional pre-processing step was implemented in this work for $R(t)$ reconstruction. More specifically, the overall fatality rate and ICU admission rate against confirmed cases are estimated well within the global values from other countries with similar incident intensity (cases per 100,000 of population) and COVID-19 testing policies (1). Therefore, since all Deaths $D(t)$ and ICU admissions are confirmed and logged with proper procedures in hospitals, these can be reasonably considered a reliable baseline for both $I(t)$ and $R(t)$ assessment in terms of data quality, under-reporting rates and subsequent missing values. It should be noted that active infections are calculated as $a.I(t) = I(t) - \hat{R}(t)$, i.e., a reliable estimation of $R(t)$ is still required even if $I(t)$ (cumulative) is accurate. Since ICU admissions related to COVID-19 per-country are not readily available in most data sources today in order to make proper statistical comparisons for Greece, $D(t)$ was used as the baseline for estimating $\hat{R}(t)$ within the no-reporting periods. In practice, every single-day official reporting of $R(t)$ is used as a reference point and high-quality interpolation against $D(t)$, specifically a spline-like piecewise cubic Hermite interpolating polynomial ('pchip') (17, 18), is employed for estimating the intermediate missing values for $R(t)$.

Figure 8 presents the interpolation process of $\hat{R}(t)$ against $D(t)$, illustrating the reference points (circles) interpolated with linear (blue), quadratic spline (magenta) and 'pchip' (red) functions; the third is chosen in this work as the best interpolator for its shape-preserving properties (16). Additionally, in Figure 9 the $R(t)$ series is interpolated directly against time (t), where there are some points where the 'pchip' interpolator is non-smooth (non-differentiable) (19, 20), hence the need to design a similar process against $D(t)$ instead. For additional quality assessment, Figure 10 presents a similar process for the $D(t)$ series against time (t), also fitted with several interpolators, namely linear (blue), logistic (green), quadratic spline (magenta) and 'pchip' (red). In this case, 'pchip' interpolator is again marginally better than quadratic spline due to its shape-preserving properties (16).

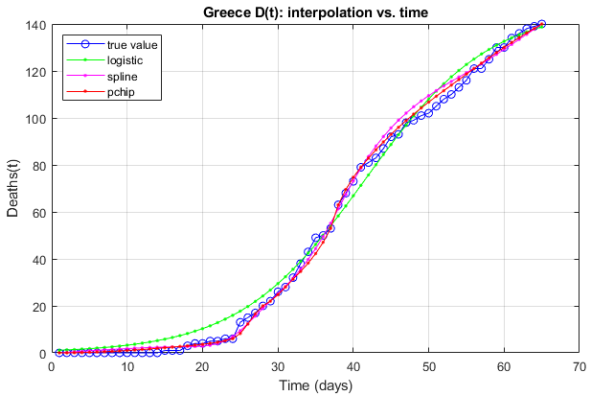

Fig. 10. Interpolation of Deaths $D(t)$ against time (t).

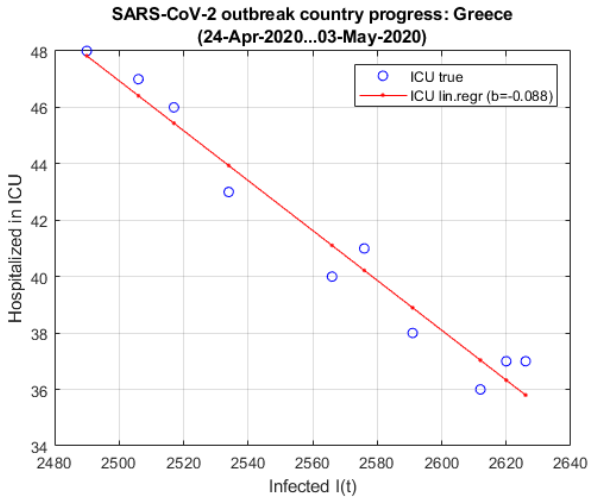

Fig. 11. Progress of the (estimated) ICU rate for Greece, according to the current 10-day LR approximation against $I(t)$.

The long-term ratio $D(t)/I(t)$ of Deaths per Infection, at 4.77% (126 in 2642) on May 5th, is more or less the same compared to the April 14th update (4.65%) and continues to reside within the reference values 2% to 5% that is estimated internationally for COVID-19 from studies for other countries (9, 21).

C. ICU admissions. One of the most important factors in the efficient management of an epidemic is the rate of ICU admissions in the hospitals and the saturation level with regard to the total number available country-side. Reports from the National Public Health Organization of Greece have stated that the initial number of 565 ICU gradually increased to at least 1,000 by mid-April. From the start of the national outbreak up to its peak in infections, Greece has been far below its saturation point, with 93 ICU beds or about 1 in 6 (at least) on April 5th. Fortunately, the ICU trend in Greece continues to be decreasing since its peak and especially since mid-April. As Figure 11 shows, the current estimation of the ICU-to-$I(t)$ ratio has a steady negative 10-day LR slope (-0.088), twice as large in magnitude compared to its previous value (-0.044) in the April 14th update (1).

On the other hand, it is difficult to make accurate estimations ratios like ICU-versus-Infections or ICU-versus-Deaths,

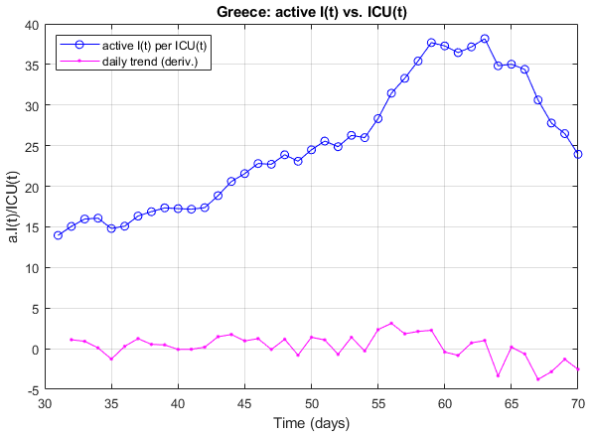

Fig. 12. Progress of the active Infections versus ICU ratio (blue) and its 1st derivative (magenta).

since the official daily reports refer only to active ICU (currently used) and cumulative exits from ICU[§§], while there is also no direct association to the final outcome, i.e., exactly what portion moves to Recovered $R(t)$ and Deaths $D(t)$. This means that the available ICU series can be associated only with the active $I(t)$ but not the cumulative $I(t)$.

Using the restored version $\hat{R}(t)$ as previously described in section 4.B, the active infections can be estimated as $a.I(t) = I(t) - \hat{R}(t)$. Then, active infections $a.I(t)$ per active ICU can be created in order to track its progression as the outbreak evolved before and after its peak infections. Figure 12 illustrates this series (blue), together with its 1st derivative (magenta) as daily trend; low values of this ratio translate to more ICU beds used per confirmed infection (worse), while high values translate to less ICU beds used per confirmed infection (better).

D. Phase differences. The plot in Figure 12 may initially seem counter-intuitive: the rate of which an active infection may led to ICU might follow the rising trend of active infections towards the peak of the outbreak. On the contrary, the plot shows almost the opposite, with *less* ICU beds required per active infection as the curve presents a local maximum somewhere between days offset 59-63. This is actually common in many epidemics, due to (a) high increase rate of confirmed infections as the outbreak moves towards its peak and (b) 'phase' difference between initial reporting of an infection and its subsequent admission to ICU after a few days when the disease progresses to worse.

In order to investigate the phase difference between the predominant epidemic data series, i.e., Recovered $R(t)$ and Deaths $D(t)$ versus Infections $I(t)$, Dynamic Time Warping (DTW) (13, 14) with Euclidean distance was employed as in section 3.A. In practice, two such data series are 'aligned' not only in the temporal but in both axes and the DTW *optimal warping path* is analyzed in order to establish the actual 'phase' difference. This is accomplished by estimating the linear regressor (LR) (15, 22) between the values of the DTW optimal warping path per-axis, according to the standard LR formulation as described in Eq.2, Eq.3 and Eq.4:

[§§] According to the NPHO-Greece daily briefing, as of May 6th the number of patients that have exited ICU was 81 in total. – https://is.gd/5yXiZ5

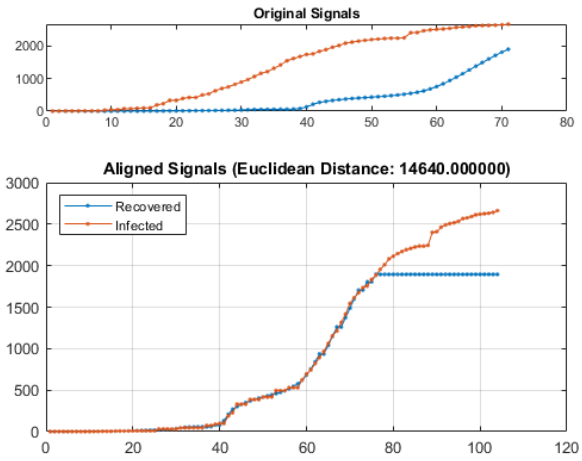

Fig. 13. DTW-based estimation of 'phase' difference of Recovered $R(t)$ versus Infected $I(t)$ ($T^{dtw}_{R,I} = 12.35$ days).

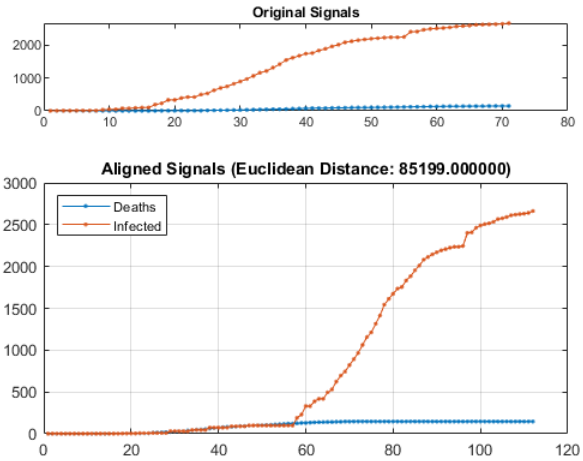

Fig. 14. DTW-based estimation of 'phase' difference of Deaths $D(t)$ versus Infected $I(t)$ ($T^{dtw}_{D,I} = 11.52$ days).

$$\hat{y}_i = \hat{b}_1 x_i + \hat{b}_0 \quad [2]$$

$$\hat{b}_1 = \sum_{i=1}^{n} \frac{(x_i - \bar{x})(y_i - \bar{y})}{(x_i - \bar{x})^2} \quad [3]$$

$$\hat{b}_0 = \bar{y} - \hat{\beta}_1 \bar{x} \quad [4]$$

where $\bar{x} = E[x] = {}^1/_n \Sigma_{i=1}^n x_i$ and $\bar{y} = E[y] = {}^1/_n \Sigma_{i=1}^n y_i$.

Then, DTW 'phase' difference can be estimated as the value $-\hat{b}_0$, i.e., the negative of the y-axis intercept point. In other words, the constant coefficient (y-axis offset) of the best-fit linear correlation between the optimal warping paths indicates the optimal 'lag' between the two data series.

Using this DTW-based approach, Figures 13 and 14 present the optimal matching paths and the matched curves for $R(t)$ versus $I(t)$ and $D(t)$ versus $I(t)$, respectively. The recovered 'phase' differences is $T^{dtw}_{R,I} = 12.35$ days for the first and $T^{dtw}_{D,I} = 11.52$ days for the second, i.e., the corresponding time period between confirmed infection and recovery or death. The $T^{dtw}_{R,I}$ value is difficult to compare to other countries, mostly due to incomplete or severe late-reporting of $R(t)$ similarly to Greece (see section 4.B). The $T^{dtw}_{D,I}$ value is somewhat lower than the estimations of 20 ± 10 days reported by other studies in China (21), but it is still within the statistically significant (p=0.95) confidence interval, i.e., compatible to what is expected.

5. Modelling the epidemic

For a more in-depth analysis of the basic data curves $I(t)$, $D(t)$ and $R(t)$ of the COVID-19 epidemic in Greece, the corresponding time series were investigated in terms of linear and periodic trends, i.e., analyze them into their primary frequency components (1).

One of the most important factors, regardless of the long-term approximation of the underlying system, is the analysis of the step-wise dependencies between successive data points, especially the confirmed cases $I(t)$. In statistical terms, this is done by estimating the auto-correlation in the time series for various lags, which produces a quantitative description of dependencies between dates, i.e., separated by a specific

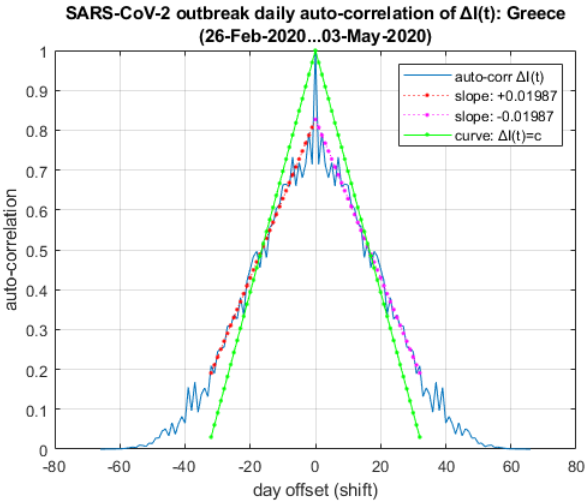

Fig. 15. Normalized auto-correlation plots of $\Delta I(t)$ (blue), the LR lines (red) in each side and the reference line (green) of the case of $\Delta I(t) = c$ (constant).

number of days. Figure 15 presents the normalized auto-correlation plot of $\Delta I(t)$ (blue), i.e., the daily increases of $I(t)$. Compared to the same plot in the previous status update on April 14th (1), it is evident here that the two sides of the lobe are almost entirely linear and the LR lines (red) in each side. Additionally, they seem to have become more 'flattened' compared to the reference line (green) that corresponds to the case of $\Delta I(t) = c$, i.e., for constant daily increase of $I(t + \tau) = c\tau + I(t)$. There is also a distinct narrow band in the central part, which indicates an even stronger correlation between successive values, i.e., more stable and 'linearized' evolution. This proves that, at least in asymptotic behaviour towards the current state, $I(t)$ increase in Greece is gradually becoming linear, even more than 2-3 weeks ago.

Another way to track the periodic 'bursts' of newly reported infections as they are reported on a daily basis is to track the changes in the short-term slope of $\Delta I(t)$. Instead of approximating the entire $I(t)$ curve as in Eq.1 for estimating the long-term behaviour, a short-term temporal window can be used to approximate the LR slope of $I(t)$ as it progresses, i.e.,

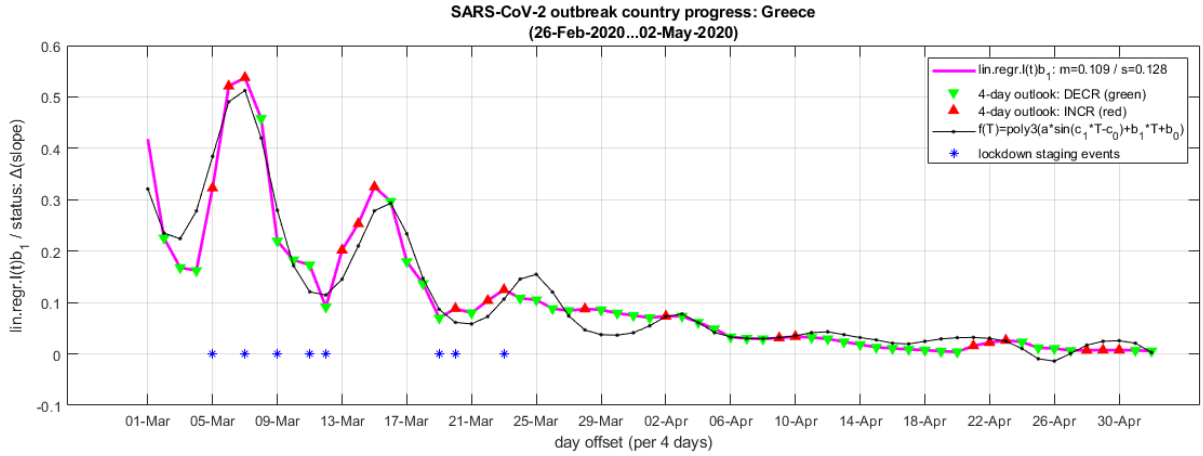

Fig. 16. 4-day sliding window slope $\hat{b}_1$ of $\Delta I(t)$ (magenta), annotations of increasing/decreasing daily trends (red/green) and LSE-fitted approximation of the $\hat{b}_1$.

the amplitude and sign of $\Delta I(t)$ changes over few subsequent days. Figure 16 illustrates such a short-term tracking of $\Delta I(t)$ via the 1st-order differential $^{d\log\hat{b}_1(t)}/_{dt}$ of LR slope of $I(t)$ with $\hat{b}_1$ as defined in Eq.3, or in other words the $\Delta^2 I(t)$, over a short-term sliding window of four days.

The main curve (magenta) in Figure 16 is the short-term LR slope $\hat{b}_1$ value for $I(t)$ as it evolves; the arrow annotations indicate decreasing (green) or increasing (red) trends; the asterisks (blue) on the x-axis indicate the major events regarding the activation of mitigation measures in Greece as described in the timeline in section 2 and in the previous update on April 14th (1). Finally, the asymptotically fading sinusoid (black) is a LSE-fitted approximation of $g_(t)$ by $\hat{g}(t)$, as defined by Eq.5, Eq.6 and Eq.7.

$$g(t) = \frac{d\log\hat{b}_1(t)}{dt} \quad [5]$$

$$\hat{g}(t) = poly3(z(t)) = \sum_{k=0}^{3} p_k z(t)^k \quad [6]$$

$$z(t) = \alpha_2 \sin(\alpha_1 t - \alpha_0) + (\beta_1 t + \beta_0) \quad [7]$$

The LSE-optimal parameters of this multi-level approximation are presented in Table 2. The upper half contains the values estimated in the previous update, while the bottom half the values estimated with data up to and including May 3rd.

Similarly to the previous update on April 14th (1), the approximation curve in Figure 16 clearly indicates three major factors: (a) periodic trend, captured by the first part of Eq.7 with α_i parameters, (b) linear decreasing trend, captured by the second part of Eq.7 with β_j parameters, and (c) asymptotically fading trend, captured by the 3rd-degree polynomial of Eq.6 with p_k parameters. Based on the comparison of the LSE-optimal parameter values in Table 2, there are two distinct differences in the current update. First, the periodic parameter α_1 that is now much smaller. Second, the current polynomial coefficients p_3 and p_2 are now of same sign and with a much smaller 3rd-degree factor, which typically indicate smoother and slower-rising derivatives. The periodic trend parameters, more specifically the $\alpha_1 = 0.466$, can be translated from radians to daily temporal range via $^{\alpha_1}/_{2\pi} = {}^{t}/_{T}$ where $T = 68d$ is the length of the data series (May 3rd) since the first confirmed infection case (February 26th), hence yielding a period

Table 2. LSE-optimal function parameters in Eq.6 and Eq.7 for Greece.

Parameter	optim.value	conf.interval
α_2	0.070	(0.040, 0.100)
α_1	0.713	(0.681, 0.745)
α_0	0.003	(-0.978, 0.985)
β_1	-0.008	(-0.020, 0.004)
β_0	0.359	(0.128, 0.590)
p_3	19.330	(11.220, 27.440)
p_2	-3.575	(-7.223, 0.074)
p_1	0.430	(0.001, 0.859)
p_0	0.044	(0.025, 0.063)
α_2	0.017	(-0.011, 0.046)
α_1	**0.466**	(0.382, 0.551)
α_0	-9.502	(-12.980, -6.024)
β_1	-0.005	(-0.017, 0.007)
β_0	0.304	(0.073, 0.535)
p_3	**4.142**	(-17.500, 25.780)
p_2	**3.022**	(-4.415, 10.460)
p_1	0.115	(-0.490, 0.720)
p_0	0.010	(-0.019, 0.039)

Note: α_0 is used with a negative sign in Eq.7. All confidence intervals are calculated for $p = 0.95$.

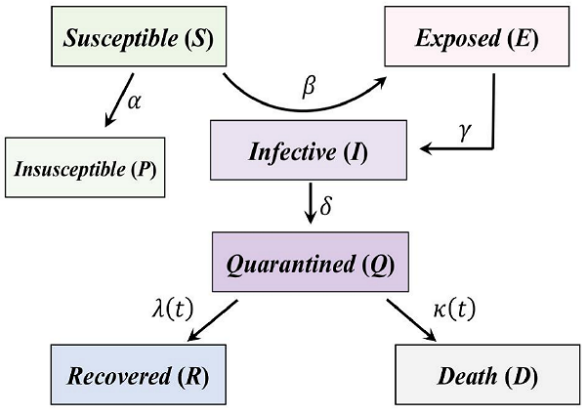

Fig. 17. The block diagram of the SEIQRDP model and its parameters.

$t_p = {}^{\alpha_1 T}/_{2\pi} \approx 0.074166T \approx 5.043d$. This is marginally smaller than the April 14th update (5.56d) and, again, coincides with the empirical data regarding the incubation (asymptomatic) period of COVID-19, estimated at 5.1-5.2 days (8, 9). Taking into consideration that the main mitigation measures (blue asterisks in x-axis) in Greece were activated just before each major 'peak' in ($\Delta I(t)$), it is re-confirmed that they were imposed in a timely manner and, thus, they were appropriate and effective in containing the 'force' of the national outbreak until today.

A. SEIQRDP model for Greece. The mathematical modelling of epidemics has been a very active research field for decades. Their main goal is to track the progress of the outbreak and its phase, in order to properly and promptly plan the mitigation measures. By far, the most popular and well-established approach is the family of *compartmental epidemic models*, originally developed as far back as 1920s. Their common characteristic is the base assumption of having a target population partitioned in *compartments* that are homogeneous in all relevant properties (e.g., sex, age, underlying pathologies, etc) and there are direct interactions between them. The three basic compartments are S='susceptible', I='infectious' and R='recovered', assuming insignificant rate of deaths and permanent immunity after recovery. Variants of this SIR base model include a D='deaths' compartment (SIRD), E='exposed' compartment (SEIR, SEIRD) for introducing an incubation period, Q='quarantined' compartment (SEIQRD, SEIQRDP) for separating the already isolated confirmed/possible carriers, etc. Based on recent models that are already being tested with COVID-19 data from China and other countries, the current work explored the epidemic data for Greece via the generic framework of a SEIQRDP model setup (23, 24). The additional P='insusceptible' corresponds to a fraction of the general population (if any) that, even when exposed to the virus, cannot become 'infected' and, thus, does not enter the E compartments and stays outside the 'pipeline' of the epidemic. More in-depth explanation of these, as well as other approaches to epidemic modelling, is included in the previous report (1).

Figure 17 illustrates the SEIQRDP model and the meaning of each parameter. The internal structure of the model, i.e., the interactions that describe the dynamics of the system, is formulated by Eq.8 through Eq.14.

Each interaction between the SEIQRDP compartments is governed by a scalar parameter that governs the way fractions of each subset is 'transferred' to another (25, 26), i.e., 'protection rate' α, 'infection rate' β, 'average latent time' γ^{-1} and 'quarantine entry rate' δ. Especially for the outflows from quarantine 'Q', the parameters are time-dependent with exponential decay functions $\lambda(t) = \lambda_0(1 - e^{-\lambda_1 t})$ with λ_0, λ_1 constants and $\kappa(t) = -\kappa_0 e^{\kappa_1 t}$ with κ_0, κ_1 constants. The full SEIQRDP model is described by the set of typical first-order linear differential equations (16) Eq.8 through Eq.14:

$$\frac{dS(t)}{dt} = -\beta\frac{S(t)I(t)}{N} - \alpha S(t) \quad [8]$$

$$\frac{dE(t)}{dt} = \beta\frac{S(t)I(t)}{N} - \gamma E(t) \quad [9]$$

$$\frac{dI(t)}{dt} = \gamma E(t) - \delta I(t) \quad [10]$$

$$\frac{dQ(t)}{dt} = \delta I(t) - \lambda(t)Q(t) - \kappa(t)Q(t) \quad [11]$$

$$\frac{dR(t)}{dt} = \lambda(t)Q(t) \quad [12]$$

$$\frac{dD(t)}{dt} = \kappa(t)Q(t) \quad [13]$$

$$\frac{dP(t)}{dt} = \alpha S(t) \quad [14]$$

In this study, the SEIQRDP model was designed based on the description of similar recent studies for other countries (24–26) and trained using the $I(t)$, $D(t)$ and $R(t)$ data series for Greece, from 26-Feb-2020 to 3-May-2020. Specifically for $R(t)$, the reconstructed interpolation-based version $\hat{R}(t)$ was used, as described previously in section 4.B. Based on this, a reconstructed version of the active infections $a.I(t) = I(t) - \hat{R}(t)$ was also generated. The purpose of this modelling was to re-estimate the general properties of SARS-CoV-2 virus and the COVID-19 outbreak on the national level, in order to: (a) confirm that the available data series are adequate and their evolution is in accordance to the research outcomes from other countries and on world-wide level; and (b) to estimate the progress of the outbreak on the mid-/long-term level, specifically for the epidemic phases, the expected peak date and magnitude, etc.

The solution of the SEIQRDP system of differential equations defined in Eq.8 through Eq.14 was estimated by a standard LSE solver (15) for iterative matching of the predicted trajectories to the real data. The software implementation was based on a heavily modified version of an open-access toolkit (27), with several improvements on convergence stability and derivatives accuracy, which deemed necessary in the early stages of the epidemic in Greece due to limited compartment sizes (small-sized populations) and severe delays in reporting $R(t)$ as described earlier.

For inclusion of a minimal under-reporting of infections, $I(t)$ data series was amplified by an additional +8% upon its recorded values. The LSE solver used centralized differential estimators, 1e-6 time step size (86.4 ms) and 1e-6 error tolerance for stopping criterion. In all cases, the process converged to a solution within less than 30 iterations, which hints that the actual epidemic data for Greece are well-described by the SEIQRDP model.

Figures 18 and 19 present the best-fit solution of the SEIQRDP model (points) and its projection (lines) until Au-

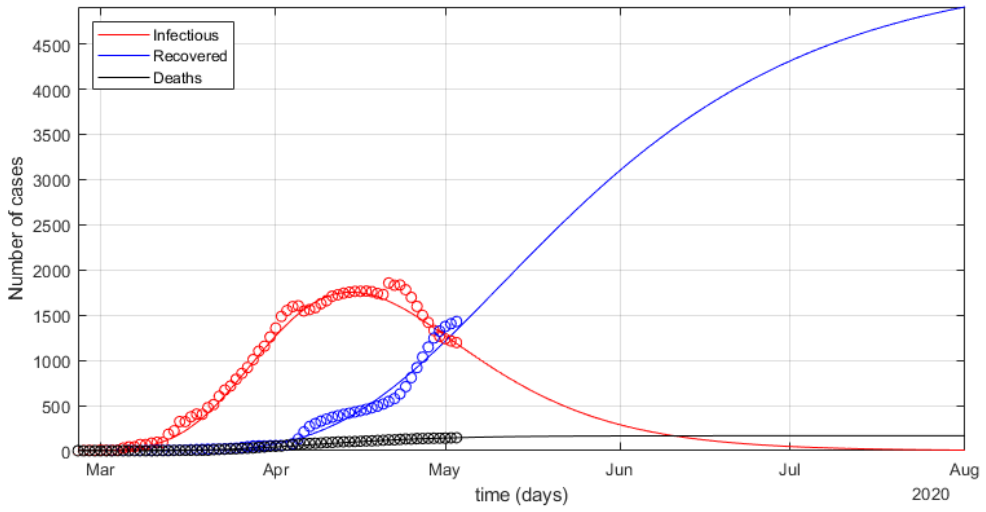

Fig. 18. SEIQRDP best-fit model (points) and its projection (lines) for $I(t)$, $D(t)$ and $R(t)$ until August (2020) in linear scale.

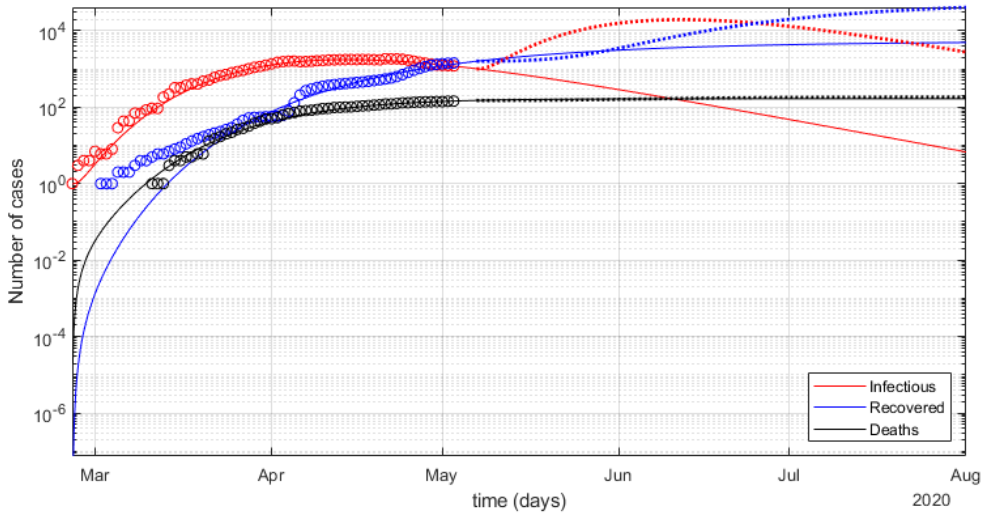

Fig. 19. SEIQRDP best-fit model (points) and its projection (lines) for $I(t)$, $D(t)$ and $R(t)$ until August (2020) in logarithmic scale.

gust (2020), in linear and logarithmic scale, respectively. The dotted line in Figure 19 illustrates the onset of a subsequent surge of the outbreak if all the mitigation measures (quarantine) was to be deactivated immediately on May 4th, but with the 'infection rate' parameter β scaled down to 1/3 of its solution in order to accommodate moderately effective social distancing and personal protection practices in the general population.

Table 3 presents the values for all the SEIQRDP parameters for the best-fit solution. The upper half contains the values estimated in the previous update, while the bottom half the values estimated with data up to and including May 3rd. It should be noted that, due to the fact that much more data are available now compared to the previous update (1) and a recovered version $\hat{R}(t)$ was used, the current SEIQRDP model fit does not include any inflation factor for $I(t)$ for addressing under-reporting effects, as previously explored. The most notable difference between the new (May 3rd) and the previous (April 14th) best-fit values is with the 'cure rate' λ parameter, now more than two orders of magnitude smaller. This updated value can be considered more reliable than the previous, since it is estimated based on more epidemic data and reconstructed $\hat{R}(t)$.

Table 3. LSE-optimal SEIQRDP model parameters in Eq.8 through Eq.14 for Greece (26-Feb-2020 to 3-May-2020), with no inflation factor for $I(t)$ under-reporting and reconstructed $\hat{R}(t)$.

Parameter	optim.value
α	0.1030
β	3.0000
γ	0.1186
δ	0.0352
λ	2.9986
κ	0.0468
α	0.0905
β	3.0000
γ	0.1114
δ	0.0638
λ	**0.0263**
κ	0.0679

Note: LSE used centralized differential estimators, 1e-6 time step size (86.4 ms), 1e-6 error tolerance for stopping criterion; convergence in 11-36 iterations; starting conditions: E_0=0, I_0=1, D_0=0, R_0=0; estimated population (2018): N_{pop}=10,724,599.

Based on the additional epidemic data available up to May 3rd and more reliable estimation of $\hat{R}(t)$, the SEIQRDP model fit provides an even better description of the outbreak characteristics in Greece compared to the April 14th update. The model essentially confirms the estimations of the outbreak peak regarding the projected dates around April 19th from very early on, even when only the first 7-10 days of April data were becoming available. The peak was realized on April 20th with $a.I(t) = 1,860$ according to the actual reported $R(t)$ or on April 21st with $a.\hat{I}(t) = 1,856$ according to the reconstructed $\hat{R}(t)$. According to the SEIQRDP model, recent data moved the projected peak of active infections about five days earlier (April 14th), but with numbers still within the expected margins of error $\Delta\{\hat{I}(t), \hat{D}(t), \hat{R}(t)\} = \{-1.26\%, -0.09\%, +13.76\%\}$ at the peak date.

It should be noted that there is temporal difference of 9-18 hours between the numbers officially reported by the Greek authority (NPHO) and the open-access datasets from John Hopkins CSSE (11), due to time zone differences and scheduled updating tasks on a daily basis. For example, $R(t) = 1,374$ was reported on April 30th and included in the CSSE datasets for Greece on May 1st. Hence, small temporal differences of $T \leq 24$ hours should be expected and considered normal. Additionally, $R(t) = 1,442$ was reported by local sources on May 3rd, but the CSSE datasets report it as $1,374$ since April 30th, until up to May 8th. More data sources will become available on the national level, as well as structured retrieval procedures and open-access APIs (12), as noted in section 3.

Summarizing the SEIQRDP model for Greece, the goodness-of-fit of the parameter solutions provides a valid 'explanation' for the dynamics of the national epidemic, i.e., the interaction between the compartments. Thus, the overall shape and scale of the corresponding curves can be considered as safe for assessments regarding the characteristics of the epidemic and its comparison to how it progresses in other countries.

B. Basic reproduction number (R_0). The availability of epidemic data for Greece beyond its peak of active infections, i.e., well past the maximum of the $I(t)$ data series, enables the estimation of a more reliable SEIQRDP model than in the previous status update on April 14th (1). Hence, the basic reproduction number R_0 can now be estimated directly from the model's best-fit parameters, instead of statistical approximations as it was presented in the previous status update (1) based in the daily progress of $I(t)$. For SEIQRDP the R_0 can be defined according to Eq.15 (25, 28, 29):

$$R_0 = \beta\delta^{-1}(1-\alpha)^t \qquad [15]$$

All parameters in Eq.15 are scalar, i.e., not including the time-dependent $\lambda(t)$ and $\kappa(t)$, but the actual estimation of R_0 is time-dependent due to the t exponent (in days). This is due to the fact that, assuming stable compartment interactions when mitigation measures are in effect (clearly after quarantine), Eq.15 describes the decay of infection rates in the population. For the best-fit SEIQRDP parameter values of Table 3 (bottom half), Eq.15 becomes $R_0 = 0.9095^t 47.022$, which estimates $R_0 < 1$ for April 24th and beyond. As mentioned earlier in section 2, during the official daily briefing on April 30th this value was reported at $0.40 < R_0 < 0.45$ and on May 4th the statement was that 'R_0 is now far below 0.5'. As Table 4 presents, the critical dates when according to Eq.15 this happened was between May 1st and 3rd, hence confirming these statements.

Table 4. R_0 estimations for Greece based on Eq.15 and best-fit SEIQRDP parameter values, using the updated epidemic data (26-Feb-2020 to 3-May-2020).

Date	R_0
May 1st	0.495
May 2nd	0.450
May 3rd	0.410

C. Under-reporting of Infections ($I(t)$). Under-reporting of the actual infections rate in the general population is a very important issue in almost every epidemic and a degradation factor for almost all analytical modelling approaches. The availability of reliable and accurate epidemic data during an outbreak, i.e., while the epidemic is evolving, is one of the most important constraints to such analytical approaches. It has to be recognized, assessed in terms of magnitude and addressed via proper pre-processing within the predictive models. One such pre-processing step is the restoration of $\hat{R}(t)$ as described previously in section 4.B.

One of the most discussed issues regarding the outbreak in Greece is the under-reporting of infections $I(t)$ and how this affects the epidemic models, as well as the confidence in planning the mitigation policies. It has been accepted by state officials that the under-reporting of $I(t)$ in Greece may be up to 20:1 (only 1 in 20 infections registered) or more, given the numbers from other countries and the targeted-only tests in Greece. A recent study[¶¶] (30) estimated the true number of $I(t)$ for Greece (mid-April) between 9,652 and 20,377 in the general population[***] rather than 2,145 officially documented by April 13th, i.e., an under-reporting rate of 6.5:1 in currently active infections. On May 3rd, the scientific committee stated that the true number of infections, including a large number of asymptomatic carriers, is probably around 20,000-30,000.

In the previous status update on April 14th (1), separate SEIQRDP models were evaluated with different assumptions regarding the extent of the under-reporting of $I(t)$. According to those models, the projected dates of peak infections ranged from April 15th to May 5th, ranging from no under-reporting ($f^I_{low} = 1.0$) to a ratio of almost 1:10 ($f^I_{high} = 9.5$), respectively. The availability of more recent epidemic data well beyond the actual peak of $I(t)$ as described previously enable the revisiting of those projections and, hence, the validity of the associated under-reporting assumptions. More specifically, the actual peak date of 20-21 of April (see above) falls between the cases April 16th ($f^I = 1.08$) or April 25th ($f^I = 4.5$). By a rough LR estimation according to Eq.2 through Eq.3, this translates to $2.60 \leq f^I \leq 2.98$, i.e., indicating under-reporting level for $I(t)$ no more than 1:3.

Additional hints regarding the under-reporting can be investigated via the Deaths $D(t)$ and ICU used compared to the infections $I(t)$ and active infections $a.I(t)$, respectively, as described in sections 4.B and 4.C. As explained previously, the $D(t)/I(t)$ fatality ratio is still within the expected zone, indicating that the overall tracking of $I(t)$, $D(t)$ and $R(t)$

[¶¶] https://imperialcollegelondon.github.io/covid19estimates/

[***] Estimated true Infected $\approx 0.13\%(0.09\%, 0.19\%)N_{pop}$ of the general population or $I(t) \approx 13942(9652, 20377)$ w.r.t. reference demographics (2018) of $N_{pop} = 10724599$ (ELSTAT).

data series are reliable enough to track the general progress of the national outbreak. Assuming that Iceland and South Korea have the best random testing in massive scale, the corresponding fatality rates of 0.6% and 2.3% can be asserted as a realistic estimation for low levels of under-reporting for $I(t)$. Hence, with Greece at 5.5% and non-saturated ICU (similar operational efficiency), simple factoring hints that the under-reporting factor is somewhere between $2.39 \leq f^I \leq 9.17$, mostly towards the first based on South Korea (144 deaths) rather than Iceland (10 deaths) where the sample is too small for statistical significance.

An issue closely related to the under-reporting of infections $I(t)$ is the policy and implementation plan regarding clinical tests for the presence of the virus in symptomatic or asymptomatic population. Due to the novelty of each emerging outbreak like with the SAR-CoV-2 virus, reliable kits are almost never available promptly for large-scale testing in the general population, at least not in the first phases of rapidly increasing new infections. Various strategies have been proposed to tackle this challenge (6), ranging from sub-optimal tests of limited reliability (use plenty of tests, more than once) to proper reliable tests but with pooling protocols (sample multiple persons per single test)[†††‡‡‡]. This is still a controversial issue in which every country employs its own policies and perspective. In Greece, the NPHO has always employed policies that include limited and very targeted tests regarding the monitoring of epidemics in the general population. For example, for the seasonal flu the official reports state that under-reporting may be up to 1:1000 as a standard practice[§§§], given of course the fact there is a readily available vaccine with moderate-to-high effectiveness in terms of protection. The officials have stated that such targeted-only, limited testing is still the main strategy for SARS-CoV-2 tracking, with tests conducted only in hospitals with symptomatic individuals and with mobile units that visit specific social groups, e.g. migrant/refugee camps throughout the country.

6. Discussion

The data analytics, best-fit model parameters and projected outcomes for Greece, as presented in the previous sections, provide solid evidence that the COVID-19 outbreak at the national level can be tracked with adequate accuracy for the general assessment of the situation, including the transition through the phases of the epidemic. Despite the problems with under-reporting of infections $I(t)$ and very late reporting of recovered $R(t)$, the models show reliable evidence that the outbreak in Greece seems to have entered recession and it is evolving into deflation, as expected.

According to projections by the best-fit SEIQRDP model, presented in Figures 18 and 19, there is strong evidence that:

- the infections peak was realized in April 20th or 21st, with 1,856-1,860 active infections, depending on the true $R(t)$ (not yet available);
- the projection of total deaths related to COVID-19 by the end of July is expected to be less than 170 (currently at 151, May 10th);
- similarly, the projection of total recovered from COVID-19, counting only confirmed cases of infections, is expected to reach 5,300 or more by the end of July;
- the currently estimated basic reproduction number is $R_0 < 0.45$ and constantly dropping;
- if no second-wave outbreak is realized, the current outbreak is expected to fade out within August (less than 10 infections reported).

Based on the data analytics results for Infected, Deaths, Recovered and ICU used, Greece gradually 'synchronized' with its neighbouring countries in Europe and in the general region, while still maintaining strict mitigation measures up to May 3rd. However, as the travel bans are gradually deactivated throughout the world, a second wave of SARS-CoV-2 epidemic is expected with a very high probability, as early as October or even September, with new spreading of the virus via air travelling and cross-countries summer holidays.

Regarding the quality and reliability of the models for Greece, Deaths seems to follow a logistic ('sigmoid') function very closely, as expected, and with statistics well within the world-wide estimations. In contrast, there are severe delays in reporting Recovered, spanning to more than a week, which introduces a very strong degradation of the corresponding data series and everything that uses it, e.g. when estimating active infections from the cumulative number. Nevertheless, data restoration via proper high-quality interpolation seems to address this problem adequately, producing results compatible with the non-restored SEIQRDP model fits but with improved estimations within the 'missing value' sub-ranges for the other data analytics models. The robustness of SEIQRDP is particularly important for assessing the quality of the projections regarding the evolution of the outbreak in Greece well into summer, using the current data and mitigation measures (before deactivating them).

The effect of under-reporting of infections in Greece was investigated via various approaches, including SEIQRDP variances with inflated Infections $I(t)$, tracking of deaths $D(t)$ against $I(t)$ and tracking active ICU against both $I(t)$ and $D(t)$. The projected (April 14th) peak infections date for various under-reporting factors (1) was also assessed against the actual realization of the peak, in order to check the validity of the initial guesses. According to the latest estimations, the effective under-reporting factor seems to be no more than 1:3, at least for the clinically important cases of COVID-19. Unreported cases of patients with very mild symptoms or completely asymptomatic may be much higher, 1:10 or more, according to the official statements in Greece and studies in other countries. More realistic estimations will become available when antibody tests in the general population are implemented within the next months.

Finally, the best-fit SEIQRDP model with data up to the last day before the beginning of gradual deactivation of the strict mitigation measures (May 3rd) was employed, using an 'infection rate' parameter β scaled down to 1/3 of its best-fit solution in order to simulate some social distancing and protective measures. Based on this, a second-wave outbreak from the subsequent week can produce a new infections peak at mid-July that may reach up to more than five times the peak of the first wave (with measures still active), as Figure 19 shows. This clearly shows the importance of maintaining

[†††] https://spectrum.ieee.org/view-from-the-valley/the-institute/ieee-member-news/everybody-in-the-pool-algorithm-researchers-tackle-the-coronavirus-test-shortage

[‡‡‡] https://www.hospimedica.com/coronavirus/articles/294781273/israeli-researchers-introduce-pooling-method-for-covid-19-testing-of-over-60-patients-simultaneously.html

[§§§] https://eody.gov.gr/wp-content/uploads/2019/01/etisia_ekthesi_gripis_2018_2019.pdf

proper social distancing, personal protection measures and constant alert regarding the proper tracking of active infections in the general population.

7. Conclusion

COVID-19 constitutes a fast-pacing, world-wide pandemic that has evolved quickly into a multi-aspect international crisis. Even with proper policies and mitigation measures properly and promptly in place, tracking the outbreak even at the national level is an extremely challenging data analytics & modelling task as the event itself is still active, thus only limited and perhaps unreliable data are currently available.

In this study, Greece is the main focus for assessing the national outbreak and estimating the general trends and outlook of it. Multiple data analytics procedures, spectral decomposition and curve-fitting formulations are developed based on the data available at hand. Standard SEIQRDP epidemic modelling is applied for Greece and for the general region around it, providing hints for the outbreak progression in the mid- and long-term, for various infections under-reporting rates.

Now with more epidemic data available, the overall short-term outlook for Greece continues to be towards positive, with much higher confidence than in mid-April (1). All numbers indicate that the national outbreak is in recession that will continue to deflate well within the summer. However, the gradual deactivation of strong mitigation measures, the re-opening of international travelling and the summer holidays period require very intense and accurate tracking of the infections in Greece and every other country, in order for the policy makers and the health infrastructure to be well-prepared for the second-wave outbreak of SARS-CoV-2 that is expected within the next months before the end of the year.

ACKNOWLEDGMENTS. The author wishes to thank every team and researcher that is currently working towards scientific works of high quality, readily accessible to the community, including technical papers, research papers and datasets. This is the only viable way to address such fast-pacing events of major world-wide impact collectively and effectively, as quickly and reliably as possible, while the crisis is still evolving.

REFERENCES

1. H Georgiou, COVID-19 outbreak in Greece has passed its rising inflection point and stepping into its peak (2020) Proofreading over the previous version 1.1.00 / 15-Apr-2020.
2. A Deslandes, V Berti, Y Tandjaoui-Lambotte, et.al., Sars-cov-2 was already spreading in france in late december 2019. *Int. J. Antimicrob. Agents* **(to appear)**, 1–11 (2020).
3. B Korber, W Fischer, S Gnanakaran, H Yoon, et.al., Spike mutation pipeline reveals the emergence of a more transmissible form of sars-cov-2. *bioRxiv (preprint)* (2020).
4. D Cyranoski, Profile of a killer: the complex biology powering the coronavirus pandemic. *Nature* **581**, 22–26 (2020).
5. F Wu, A Wang, M Liu, Q Wang, Neutralizing antibody responses to sars-cov-2 in a covid-19 recovered patient cohort and their implications. *medRxiv (preprint)* (2020).
6. M Esbin, O Whitney, S Chong, et.al., Overcoming the bottleneck to widespread testing: A rapid review of nucleic acid testing approaches for covid-19 detection. *Cold Spring Harb. Lab. Press.*, 1–22 (2020).
7. C Wang, W Li, D Drabek, et.al., A human monoclonal antibody blocking sars-cov-2 infection. *Nat. Commun.* **2251**, 1–6 (2020).
8. S Lauer, K Grantz, Q Bi, F Jones, et.al., The incubation period of coronavirus disease 2019 (covid-19) from publicly reported confirmed cases: Estimation and application. *Annals Intern. Medicine* (2020).
9. A Kucharski, T Russell, C Diamond, et.al., Early dynamics of transmission and control of covid-19: a mathematical modelling study. *The Lancet Infect. Dis.* (2020).
10. B Maier, D Brockmann, Effective containment explains sub-exponential growth in confirmed cases of recent covid-19 outbreak in mainland china. *medRxiv (preprint)* (2020).
11. E Dong, H Du, L Gardner, An interactive web-based dashboard to track covid-19 in real time. *The Lancet Infect. Dis.* (2020).
12. CR Greece, Coronavirus greece api: A simple and fast api for tracking the coronavirus (covid-19) outbreak in greece (2020).
13. E Keogh, C Ratanamahatana, Exact indexing of dynamic time warping. *Knowl. Inf. Syst.* **7**, 358–386 (2005).
14. T Rakthanmanon, Addressing big data time series: Mining trillions of time series subsequences under dynamic time warping. *ACM Transactions on Knowl. Discov. from Data* **7**, 10:1–10:31 (2013).
15. S Theodoridis, K Koutroumbas, *Pattern Recognition*. (Academic Press), 4th edition, (2008).
16. M Spiegel, J Liu, S Lipschutz, *Mathematical Handbook of Formulas and Tables (4th/Ed.)*. (McGraw-Hill), (2012).
17. F Fritsch, R Carlson, Monotone piecewise cubic interpolation. *SIAM J. on Numer. Analysis* **17**, 238–246 (1980).
18. D Kahaner, C Moler, S Nash, *Numerical Methods and Software*. (Prentice Hall, Upper Saddle River, NJ, USA), (1988).
19. M Hazewinkel, *Encyclopedia of Mathematics*. (Springer / Kluwer Academic Publishers), (2001).
20. S Bronshtein, *Handbook of Mathematics*. (Springer), 4th edition, (year?).
21. J Wu, K Leung, M Bushman, N Kishore, et.al., Estimating clinical severity of covid-19 from the transmission dynamics in wuhan, china. *Nat. Medicine Lett.* (2020).
22. M Spiegel, J Schiller, R Srinivasan, *Probability and Statistics (3rd/Ed.)*. (McGraw-Hill), (2009).
23. E Piccolominib, F Zamaa, Preliminary analysis of covid-19 spread in Italy with an adaptive seird model. *arXiv:2003.09909v1 [q-bio.PE]* (2020).
24. L Peng, W Yang, D Zhang, C Zhuge, L Hong, Epidemic analysis of covid-19 in China by dynamical modeling. *arXiv:2002.06563v1 [q-bio.PE]* (2020).
25. R Leipus, O Stikonien, Apibendrinto seir modelio taikymas covid-19 ilgalaikems prognozems. *VU, Taikomosios Matematikos Institutas*, 1–5 (2020).
26. M Bahloul, A Chahid, TM Laleg-Kirati, Fractional-order seiqrdp model for simulating the dynamics of covid-19 epidemic. *arXiv:2005.01820v1*, 1–11 (2020).
27. E Cheynet, Generalized seir epidemic model (fitting and computation) (2020).
28. X Bardina, F Ferrante, C Rovira, A stochastic epidemic model of covid-19 disease. *arXiv:2005.02859v1*, 1–14 (2020).
29. P Driessche, Reproduction numbers of infectious disease models. *Infect. Dis. Model.* **2**, 288–303 (2017).
30. S Flaxman, S Mishra, A Gandy, et.al., Estimating the number of infections and the impact of nonpharmaceutical interventions on covid-19 in 11 european countries. *Imp. Coll. Lond. (UK), COVID-19 Response Team* (2020).